The 2017 Cold-Pool Exchange Process Study supporting the Utah Wintertime Fine Particulate Study (UWFPS)

Sebastian W. Hoch and Erik T. Crosman
Department of Atmospheric Sciences
135 S 1460 E, Rm 819
University of Utah
Salt Lake City, UT 84112-0110

Final Report prepared for the
Utah Division of Environmental Quality

Summary

While vertical and horizontal mixing is largely inhibited within Utah's persistent wintertime cold-air pools (PCAPs) and emissions of particulate pollution and precursor gases accumulate to form extensive pollution episodes, some meteorological processes can still modulate their concentrations. These cold-air pool Exchange Processes, comprising thermally driven circulations (diurnal mountain winds and the lake breeze), weak air-mass boundaries, and terrain-forced flows, were targeted by a small experiment in January and February 2017 to augment the Utah Wintertime Fine Particulate Study (UWFPS). The results of this study, summarized in this report, include the identification of influences of down-valley flows on concentrations of both particulate matter and ozone, and highlight the large pollution gradients that can result from boundary-layer airmass exchanges between the Great Salt Lake and Salt Lake Valley.

Table of Contents

1. Introduction

1.1 Background

The Salt Lake Valley (SLV) and other Utah basins experience persistent cold-air pool (PCAP) episodes under high-pressure synoptic conditions during the wintertime (Lareau et al. 2013, Whiteman et al. 2014). Under the stable atmospheric PCAP conditions, vertical mixing is inhibited and particulate pollutants accumulate and affect the population along the Wasatch Front. Typical winters see exceedances of the National Ambient Air Quality Standard for PM2.5 on 18 days during an average of 6 multi-day pollution episodes (Whiteman et al. 2014). A major field study funded by the National Science Foundation, the Persistent Cold-Air Pool Study (PCAPS), was conducted in the SLV in 2010-2011. The goals of PCAPS were to improve understanding of the meteorological formation, maintenance, and decay of cold-air pools (Lareau et al. 2013). PCAPS data and subsequent scientific analysis resulted in improved understanding of PCAP boundary-layer structure and climatology of wintertime particulate pollution in the SLV (Silcox et al. 2012, Whiteman et al. 2014, Whiteman and Hoch 2014, Young and Whiteman 2015, Crosman and Horel 2016), improved understanding of the interactions between synoptic weather systems and PCAP events (Lareau and Horel 2015a, Lareau and Horel 2015b), and improved numerical simulations of PCAP episodes (Lu and Zhong 2014, Foster et al. 2016, Crosman and Horel 2017). The following meteorological ingredients, of which only some may be present during any given PCAP, have been found to play an important role in the lifecycle of PCAPs (Lareau et al. 2013):

PCAP formation and maintenance mechanisms

- Cold-air emplacement in the Great Salt Lake Basin from a cold low pressure system prior to PCAP onset;
- High pressure and associated subsidence temperature inversion that initially forms above mountaintop and descends over time;
- Deep snow cover and resulting enhanced nocturnal radiative cooling and decreased absorption of incoming daytime solar radiation at the land surface;
- Cold air from over the Great Salt Lake returning to engulf the Salt Lake Valley following partial pollution mix-out events after the passage of weak weather systems;
- Persistent stratus cloud decks that limit incoming solar radiation and redistribute radiative cooling from the surface to cloud top.

PCAP decay mechanisms:

- Synoptic westerly and southwesterly flows that slowly erode the PCAP from the top down;
- Modification of PCAP through absorption of solar radiation at the land surface;
- Cooling aloft associated with approaching storm system;
- Rapid increase in winds and decrease in temperature associated with a strong cold front (results in complete removal of PCAP in 1-2 hours).

The intensity of PCAPs is often described through the use of heat deficit (see Section 2.1). While the various meteorological ingredients associated with PCAPs are well known, the relative importance of these various factors varies from PCAP episode to episode and is difficult to quantify with limited meteorological observations during non-field study periods. In addition, the relationship and complex interactions between meteorology, flow patterns within the PCAP, and the complex chemistry in the SLV remains a major unanswered scientific question (Baasandorj et al. 2017.)

Meteorological transport and mixing processes such as horizontal and vertical advection are inhibited due to the overall stable stratification within PCAPs. Nevertheless, thermally driven flows such as downvalley and downslope, and upvalley and upslope flows (Zardi and Whiteman 2012) can be triggered by thermal contrasts within and amongst the basins and surrounding topography affected by PCAPs. Further, the thermal inertia of the Great Salt Lake results in lake breeze circulations (Lareau et al. 2013, Crosman and Horel 2016), while inter-basin thermally and pressure-driven flows resulting from slope drainages and horizontal gradients in temperature between the Utah and Salt Lake Valleys are commonly observed.

The Cold-Air Pool Exchange Processes resulting from diurnal mountain wind systems, interbasin exchange, and lake breeze circulations are often weaker under PCAP than under non-PCAP conditions. Nevertheless, they are expected to influence pollutant and precursor concentrations and thus to modify chemical processes within PCAPs.

A meteorological experiment, funded by NSF (Grant # AGS-1723337) and the Utah Department of Air Quality, was conducted in January and February 2017 to allow the characterization of Cold-Air Pool Exchange Processes and PCAP evolution and to complement the chemical observation of UWFPS.

1.2 Scope of Study

The Cold-Air Pool Exchange Study augmenting the Utah Wintertime Fine Particulate Study (UWFPS) was sponsored by the Utah Division of Air Quality (DEQ) and received additional funding from the National Science Foundation (NSF, Grant # AGS-1723337). Observations were tightly connected to observations by the other UWPFS participants from the National Oceanic and Atmospheric Administration (NOAA), Environmental Protection Agency (EPA), DEQ, and several universities.

The main goal was to investigate the role of exchange processes, and the secondary deliverable was meteorological support to UWFPS by providing daily weather forecast and outlooks for the planning of Twin Otter Research flights.

1.3 Goals of this Report

This report to UDAQ covers the observations of meteorological conditions during the air pollution episodes of the 2016-2017 pollution season. Instrumentation ranging from small inexpensive temperature data loggers deployed along an elevation-transect from the valley floor up the basin sidewall, to sophisticated remote-sensing equipment such as ceilometers and a Doppler Wind LiDAR, were used to monitor the spatial and temporal variation of the atmospheric conditions within the valley cold air pools. This report documents the observations

(location, instrumentation; Section 2), summarizes the meteorological analysis and key findings (Section 3), and forecasting for UWFPS (Section 4). More details on the entire UWFPS project are available in the UWPFS report to UDAQ.

2. Observations

The observational sites of the Cold-Air Pool Exchange Process Study are shown on a map (**Fig. 1**) of the northeastern part of the Salt Lake Valley. The site names, abbreviations, elevations, type of measurements, and site coordinates are shown in **Table 1**. The key locations for meteorological observations were Hawthorne Elementary (HW), the University of Utah William Browning Building (UU), the University of Utah Mountain Meteorology Laboratory at the mouth of Red Butte Canyon (RB), the Salt Lake City Landfill (LFL), a site near 800 S and 800 E in Salt Lake City (8th&8th), and two sites at the mouth of Parleys Canyon (PAR). Radiosondes were launched twice a day by the National Weather Service (NWS) from the Salt Lake International Airport (KSLC), and additional soundings were flows during PCAP conditions from the 8th&8th site. Small and inexpensive temperature data loggers were distributed along an elevation transect running up the northeastern sidewall of the Salt Lake Valley. Additional *mobile* observation platforms were two instrumented TRAX trains and the KSL-TV news helicopter.

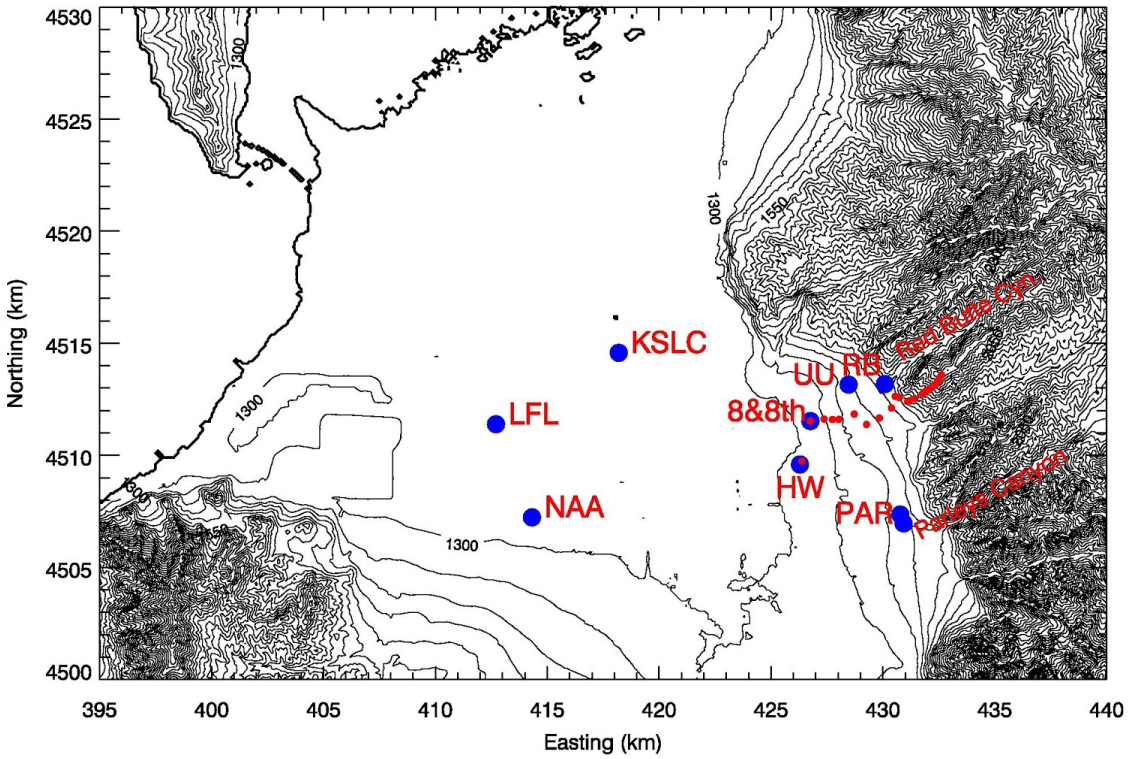

Figure 1: Map (UTM grid, 100 m elevation contours) of the northern part of the Salt Lake Valley showing the locations of meteorological observation sites. Blue dots mark sites with multiple meteorological sensors and/or profilers, as described in Table 1. Red dots mark automatic temperature data loggers deployed along an elevation transect between ~1300 m and 2150 m ASL. The thick elevation contour approximately shows the coastline of the Great Salt Lake.

Table 1: The main meteorological observational sites in the Salt Lake Valley.

Site Name	Site Abbreviation	Instrumentation	Elevation (m ASL)	Surrounding elevation (m ASL)	Elevation above ground (m)	Latitude (°N)	Longitude (°E)
University of Utah; William Browning Building	UU (base) and (top)	Temp/RH, Wind, Solar and infrared radiation, turbulence	1442 m 1465 m	1435 m	2 m and 30 m	40.766082° 40.766187°	-111.8468° -111.8477°
Hawthorne Elementary; UDAQ site	HW-LIDAR	Temp, Lidar wind profile, Ceilometer	1310 m	1307 m	2 m	40.735269°	-111.8719°
Salt Lake City International Airport	KSLC	Temp/RH, Wind, Radiosonde	1289 m	1289 m	122 m	40.772436°	-111.9547°
Mountain Meteorology Laboratory; mouth of Red Butte Canyon	RB	Temp/RH, Wind, Ceilometer, O3, PM	1522 m	1520 m	2 m	40.7666°	-111.8284°
Salt Lake Landfill	LFL	Sodar Wind Profile, Ceilometer O3, PM	1292	-	-	40.74879	-112.0340
Neil Armstrong Academy	NAA	Temp/RH, Wind, O3	1301 m	1298 m	3 m	40.71152°	-112.0145°
Parleys Canyon Exit Site 1	PAR	Sodar Wind Profiler	1388	-	-	40.71423	-111.8196
Parleys Canyon Exit Site 2	PAR	Ceilometer O3, PM	1433	-	-	40.7107	-111.8178
800 S & 800 E	8th&8th	Radiosonde during PCAP events	1311	-	-	40.75146	-111.8676

2.1 Temperature Profiles and the Valley Heat Deficit

Vertical profiles of the atmospheric temperature are necessary to evaluate static stability of the atmosphere and to help to define the strength of diurnal and persistent cold air pools. A good measure of the stability of a valley atmosphere is the Valley Heat Deficit (VHD). Two independent observations of the temperature structure in the Salt Lake Valley were made to calculate the VHD. The first observation is readily available from the twice-daily radiosonde ascents from KSLC. Radiosondes are launched daily, at approximately 0500 and 1700 MST. Additional soundings were flown during PCAP conditions from the 8th&8th site. The second observation is based on a pseudo-vertical assumption (Whiteman and Hoch 2014), where temperature observations along an elevation transect are interpreted as a proxy for the vertical

variation of temperatures within the valley or basin atmosphere. A set of 23 inexpensive temperature data loggers (Hobo© Pro v2, Onset Computers, MA) was deployed housed in 6-plate radiation shields (R. M. Young, MI) along an elevation transect. With the exception of the topmost sensor, they were deployed at a height of approximately 130 to 180 cm above the surface. Sensors in the upper basin were installed on available dead branches of the vegetation, to avoid any disturbance of the environment. The topmost sensor on the summit of Mt. Wire was installed on the top of a freely accessible tower, approximately 10 m AGL. Temperature data was recorded every 5 minutes and stored on local memory. Locations of the sensors are given in **Table 2.**

The Valley Heat Deficit (VHD) is a measurement of the amount of energy that would be needed to bring a valley or basin atmosphere to a neutral stratification. Following Whiteman et al. (1999, 2014) it is calculated for the Salt Lake Valley as

$$VHD = c_p \int_{1300\,m}^{2200\,m} \rho(z)\,[\theta_h - \theta(z)]\,dz, \quad [\mathrm{J\ m^{-2}}],$$

where θ_h is the potential temperature at height *h*, $\rho(z)$ and $\theta(z)$ are the air density and potential temperature from the twice-daily rawinsonde sounding, respectively. The specific heat of air at constant pressure is denoted as c_p, and *dz* is 10 m. The VHD is the heat required to warm an atmospheric column with a 1-m^2 base to the potential temperature observed at the top of the basin at height *h*=2200 m, bringing the underlying atmosphere to a dry adiabatic lapse rate. Calculations were performed using the twice-daily radiosondes launched by the NWS at the KSLC site, additional radiosondes launched during intensive observational periods, and based on the pseudo-vertical temperature soundings recorded along the northeastern valley sidewall. For the Salt Lake Valley, the elevation range between 1300 m ASL (valley floor) and the height of 2200 m, corresponding the mean ridge height surrounding the valley, are used. Calculations of VHD reveal the episodes of high atmospheric stability during the passage of high-pressure centers across Northern Utah.

Table 2: Locations and elevation of Hobo® automatic temperature dataloggers deployed along an elevation transect in the northeastern Salt Lake City Basin during UWFPS.

Identifier	Latitude (deg N)	Longitude (deg E)	Elevation (m ASL)	Serial number
HOBO_01	40.73528	-111.87189	1307	10538180
HOBO_02	40.75146	-111.86762	1311	9889090
HOBO_03	40.75146	-111.86762	1311	9810707
HOBO_04	40.75231	-111.86035	1338	9806339
HOBO_05	40.75216	-111.85593	1372	9806338
HOBO_06	40.75225	-111.85254	1388	9806340
HOBO_07	40.75443	-111.84443	1427	9806358
HOBO_08	40.75032	-111.83782	1429	9784026
HOBO_09	40.75292	-111.83113	1457	9826455
HOBO_10	40.75702	-111.82473	1493	978403
HOBO_11	40.7617	-111.82282	1527	980633

HOBO_12	40.76124	-111.82067	1542	980633
HOBO_13	40.7596	-111.81619	1607	9806342
HOBO_14	40.76007	-111.81534	1662	9784035
HOBO_15	40.76085	-111.81250	1716	9784034
HOBO_16	40.7628	-111.80849	1804	9806354
HOBO_17	40.76373	-111.80695	1888	9806344
HOBO_18	40.76477	-111.80495	1953	9784028
HOBO_19	40.76572	-111.80326	2000	9784029
HOBO_20	40.76664	-111.80176	2048	9784027
HOBO_21	40.76799	-111.80014	2105	9806345
HOBO_22	40.76915	-111.79947	2137	9784030
HOBO_23	40.77055	-111.79835	2181	9806343

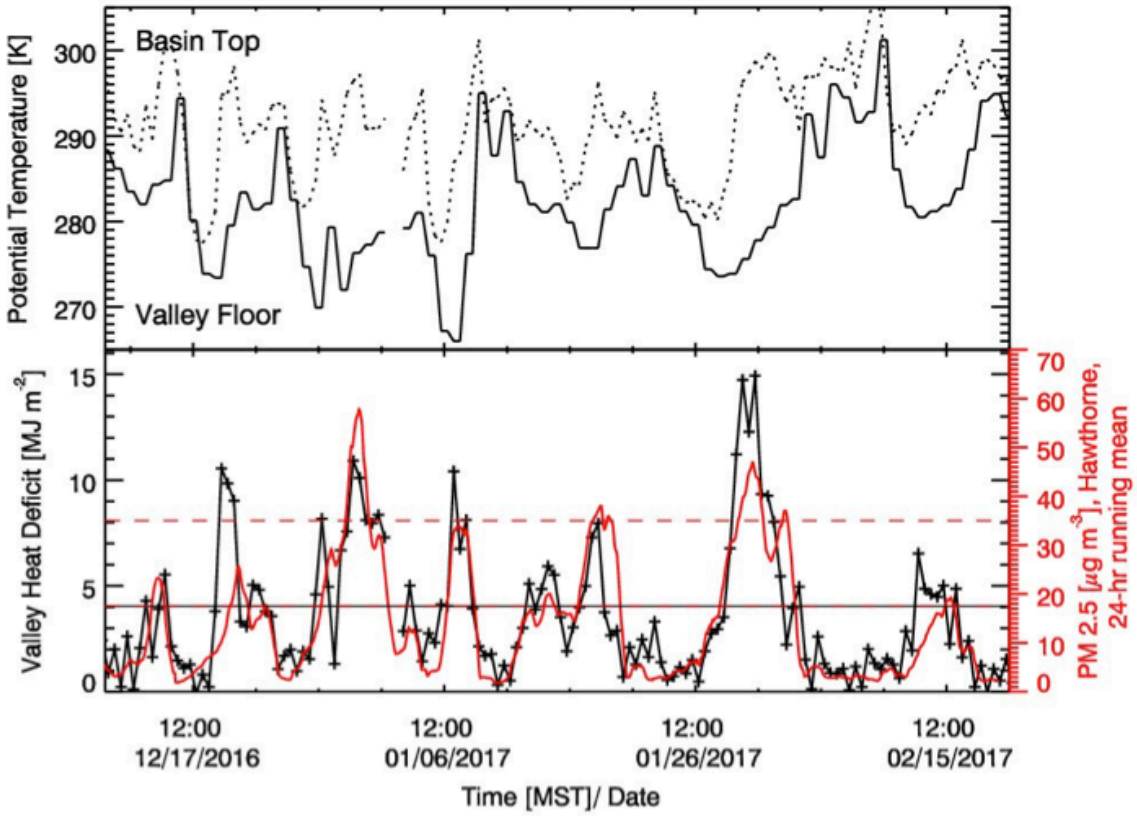

Figure 2: Potential temperature at the base and top of the Salt Lake City Basin from radiosonde observations by the National Weather Service (top), and the Valley Heat Deficit (VHD, black) and the smoothed observations of $PM_{2.5}$ pollutant concentrations (red) from the UDAQ Hawthorne (HW) site. Data covers the main observational period of the experiment, from 15 December 2016 through 20 February 2017. Note that the horizontal dashed line marks the NAAQS for $PM_{2.5}$ and the horizontal red-black dashed line marks the VHD threshold value of 4.04 MJ m^{-3} and a $PM_{2.5}$ concentration of 17.5 μg m^{-3}.

2.2 Wind Profiles

Wind profiles, while available from the radiosondes from the KSLC and 8th&8th launch sites, were also continuously recorded using the University of Utah Halo Photonics (UK) Doppler wind lidar and from two Atmospheric Systems Corporation (Santa Clarita, CA) mini-SoDARs. The lidar was installed in a backyard of a local volunteer who lives in the direct vicinity of Hawthorne Elementary (HW) site. The installation required a fixed power source and an unobstructed view of sky. The lidar was programmed to scan a Plan Position Indicator (PPI) scan pattern every 10 minutes. The Vertical Azimuth Display (VAD) analysis was used to retrieve the vertical profile of the three-dimensional wind field. This wind field can be overlaid with the aerosol backscatter coefficient of the lidar retrieval or of the co-located ceilometer. Daily quicklooks were produced during the experiment and shared via a web page with the collaborators and interested public.

The two SoDARs were installed at the LFL and PAR sites, recording 10-min average wind profiles up to 200 m AGL with a vertical resolution of 10 m. Regular maintenance was necessary to keep the PAR site sodar running, as it was powered by solar power and snow had to be removed from the antenna housing.

2.3 Aerosol Backscatter

Aerosol backscatter profiles were recorded with three ceilometers at three locations in the Salt Lake Valley to resolve spatial differences in the atmospheric aerosol loading and to resolve temporal changes in the aerosol optical properties at these three sites. Ceilometers (Vaisala CL31), were deployed at the Salt Lake Landfill (LFL), at the mouth of Parleys Canyon (PAR), and the Red Butte Canyon Exit (RB) sites. These observations complement the observations at Hawthorne (HW) and in the Utah and Cache basins made with the EPA deployed Vaisala CL51 ceilometer. The instruments recorded a vertical profile (10-m resolution) of the atmospheric aerosol backscatter coefficient β every 16 seconds. The raw data was averaged to 10-min means for further processing. Daily quicklooks (see **Fig. 3** as example) are available for the experiment at the following web site: http://www.inscc.utah.edu/~hoch/AIRQUAL_2016-2017/CEILOMETER/. Time-height cross sections of aerosol backscatter illustrate changes in the polluted PCAP atmosphere, and visualize mixing processes, layering, and injection of clean air along basin sidewalls or through tributary canyons. Further, phases of quickly intensifying backscatter retrievals may indicate periods of $PM_{2.5}$ formation.

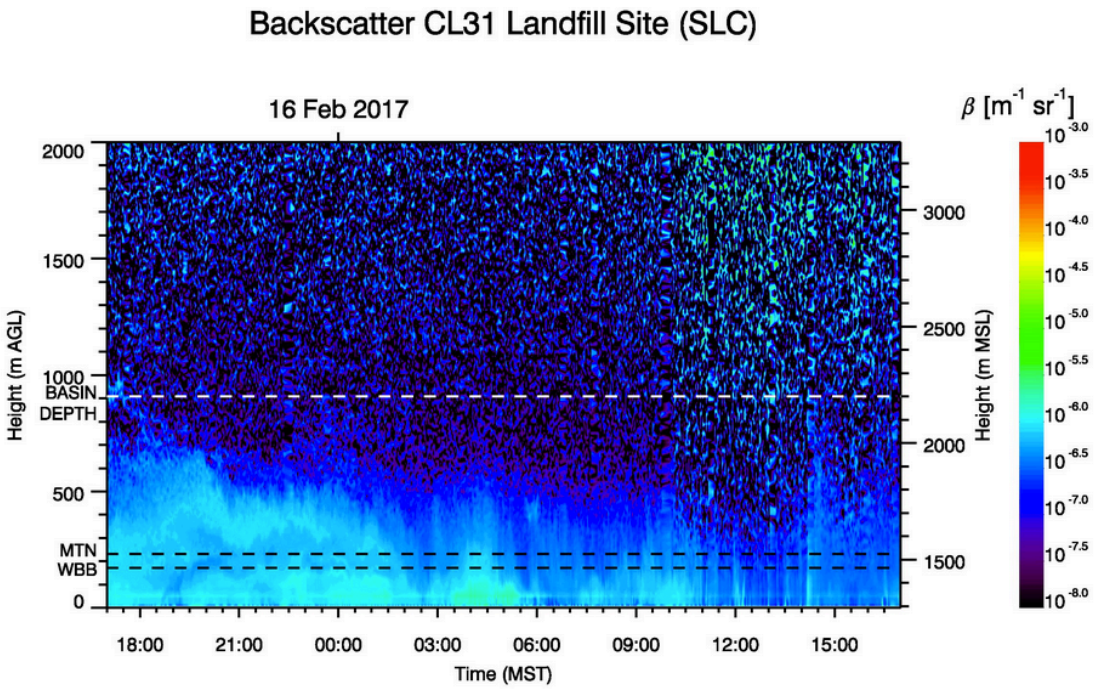

Figure 3: Example quicklook product showing the ceilometer retrieved vertical profile of the aerosol backscatter coefficient (β) at the Landfill (LFL) site.

2.4 Chemical observations co-located with meteorological equipment

Observations at the LFL, PAR and RB sites were co-located with ozone and particulate concentration measurements.

The $PM_{2.5}$ measurements were recorded by two types of research-grade laser nephelometers manufactured by Met One Instruments: The E-Sampler 9800 or the ES-642 monitors [precision: 3 µg/m^3, uncertainty: 8%] with sharp cut cyclones at the inlet to restrict particle size sampled to $PM_{2.5}$ or smaller. The E-Samplers and ES-642 monitors are calibrated by the manufacturer and have been shown to compare well in match-ups between DAQ measurements.

The ozone measurements were recorded by a Model 205 Dual Beam Ozone Monitor (O3) from 2B Technologies, CO, [precision: 2% uncertainty: 2%]. The 2B Ozone Monitor utilizes UV absorption at 254 nm and is approved by EPA as a Federal Equivalent Method (FEM). The 2B Ozone Monitors were calibrated against DAQ standards as well as a 2B Technologies Model 306 Calibration Source.

2.5 Turbulence Intensity and Vertical Mixing

Turbulence kinetic energy (TKE) is a measure of turbulence intensity. To evaluate the strength of atmospheric mixing at the valley sidewall (UU) site, turbulence observations were made using a Campbell Scientific CSAT3 ultrasonic anemometer to measure the three-dimensional wind field at 20 Hz. This dataset was processed using the Utah Turbulence in Environmental Studies processing and analysis code (UTESpac).

A second measure of atmospheric mixing and turbulence is the vertical velocity variance (σ_w) that was derived from vertical stare data collected with the University of Utah Doppler wind lidar.

2.6 Solar and Infrared Radiation

Solar incoming and reflected radiation was measured at the University of Utah (UU) site, using pyranometers (CMP21, Kipp and Zonen, Delft, the Netherlands) and in- and outgoing thermal (longwave) radiation were monitored with pyrgeometers (CGR4, Kipp and Zonen, Delft, the Netherlands). Observations of solar radiation can indicate the degree of cloudiness and the amount of radiative energy available to drive photochemical reactions. The surface albedo - the ratio between reflected solar and incoming solar radiation - indicates the surface conditions such as the degree snow cover or bare grass surface. Changes in infrared incoming radiation indicate the degree of cloud cover and cloud height, while the outgoing longwave radiation is a function of surface temperature and emissivity.

2.7 Basic Weather Observations

Basic weather observations (temperature and relative humidity, pressure, wind speed and direction) are available for many location throughout the Salt Lake Valley via MesoWest (Horel et al. 2002; see mesowest.utah.edu), and could be retrieved for the Neil Armstrong Academy (NAA), University of Utah rooftop (UU), Red Butte Canyon Exit (RB), etc. Basic meteorological data in high temporal resolution from Hawthorne (HW) was received from Utah Division of Air Quality.

2.8 Mobile Observation Platforms

Besides the surface-based and remote sensing platforms, two datasets from mobile platforms were available during the experiment. These were deployed and maintained by unfunded collaborators who were willing to share their datasets. The mobile platforms consisted of two TRAX trains operated by the Utah Transit Authority (UTA) and the local news helicopter operated by KSL-TV, and were equipped with $PM_{2.5}$ concentration monitors.

3. The January and February 2017 Pollution Episodes

January and February 2017 were characterized by above-average precipitation in northern Utah associated with several active storm track periods during these months (5.0 cm observed in January versus normal of 3.2 cm, 4.3 cm in February versus normal of 3.2). These active storm tracks resulted in less frequent PCAP conditions than is climatologically observed. However, two dominating episodes of the 2016-2017 winter occurred during the UWFPS period when the NOAA Twin Otter was deployed in Utah: 13 - 20 January 2017, and 27 January - 4 February 2017 as shown **Fig. 2**. Temperatures were below normal in January associated with the active storm track (mean January temperature of 27.15 F versus normal of 29.75 F). In February, warm storms and periods of high pressure without snow cover resulted in higher temperatures than average (39.95 F versus normal of 34.2 F).

Snow cover is an important variable in PCAP occurrence and strength (**Table 3**). The Cache Valley saw the deepest and most persistent snow cover during the January-February 2017 period.

Table 3: Snow depth (inches) every three days in the three valleys during January 15th - February 15th (source cocorahs.org)

Date	Salt Lake Valley	Utah Valley	Cache Valley
Jan 15th	0-1”	0	7-9”
Jan 18th	0	0	6-8”
Jan 21st	4-10”	2-4”	10-12”
Jan 24th	4-8”	2-4”	21-27”
Jan 27th	3-8”	2-4”	19-24”
Jan 30th	3-7”	NA	18-22”
Feb 2nd	1-5”	1-3”	18-20”
Feb 5th	0”	0”	11-15”
Feb 8th	0”	0”	6-12”
Feb 11th	0-1”	0”	3-8”
Feb 14th	0”	0”	1-3”

Meteorological summaries of the two primary episodes of the UWFPS study in the Salt Lake Valley follow.

3.1 13 January – 21 January 2017

The pollution layer observed in this 13 January – 21 January 2017 PCAP was between 400 – 800 m deep, which is significantly deeper than the typical mean pollution layer depth of ~400 m for PCAPs in the Salt Lake Valley derived from ceilometer backscatter (Young and Whiteman 2014) (**Fig. 4**). The factors contributing to the ‘non-classical’ behavior of this PCAP were a lack of snow cover, the relatively weak subsidence inversion with a reduces capping stability, thick clouds and associated vertical mixing below the cloud base during more than half of the episode. Wind speeds aloft remained light during this episode until strong southwesterly flow ahead of two strong storm system resulted in top-down erosion of the CAP beginning on 19 January.

3.4 26 January – 3 February 2017

This 26 January – 3 February 2017 episode was a classic PCAP, with an onset marked by cold air left in place by a storm system and several inches of fresh snow on the ground, followed by a large high pressure ridge over the Western USA. A subsidence inversion associated with the high pressure system descended from ~1200 m AGL on 27 January to near 400 m AGL by 1 February (**Fig. 4**). This capping layer confined the pollution layer below the base of the descending stable layer, as illustrated by ceilometer backscatter. A period of low clouds developed in the Great Salt Lake Basin and Salt Lake Valley in the middle of the episode (30 January – 1 February), decreasing nighttime stability and increasing sub-cloud turbulent mixing.

Winds above the stable layer at 700 hPa were generally light from 27 January – 30 January, but increased above 10 m s^{-1} from the 31st January until the end of the episode, eroding the polluted stable layer in the Salt Lake Valley to only 100-200 m by the 3rd of February. Airmass exchanges with the Great Salt Lake complicated the end of the episode in the Salt Lake Valley (see Section 4.4).

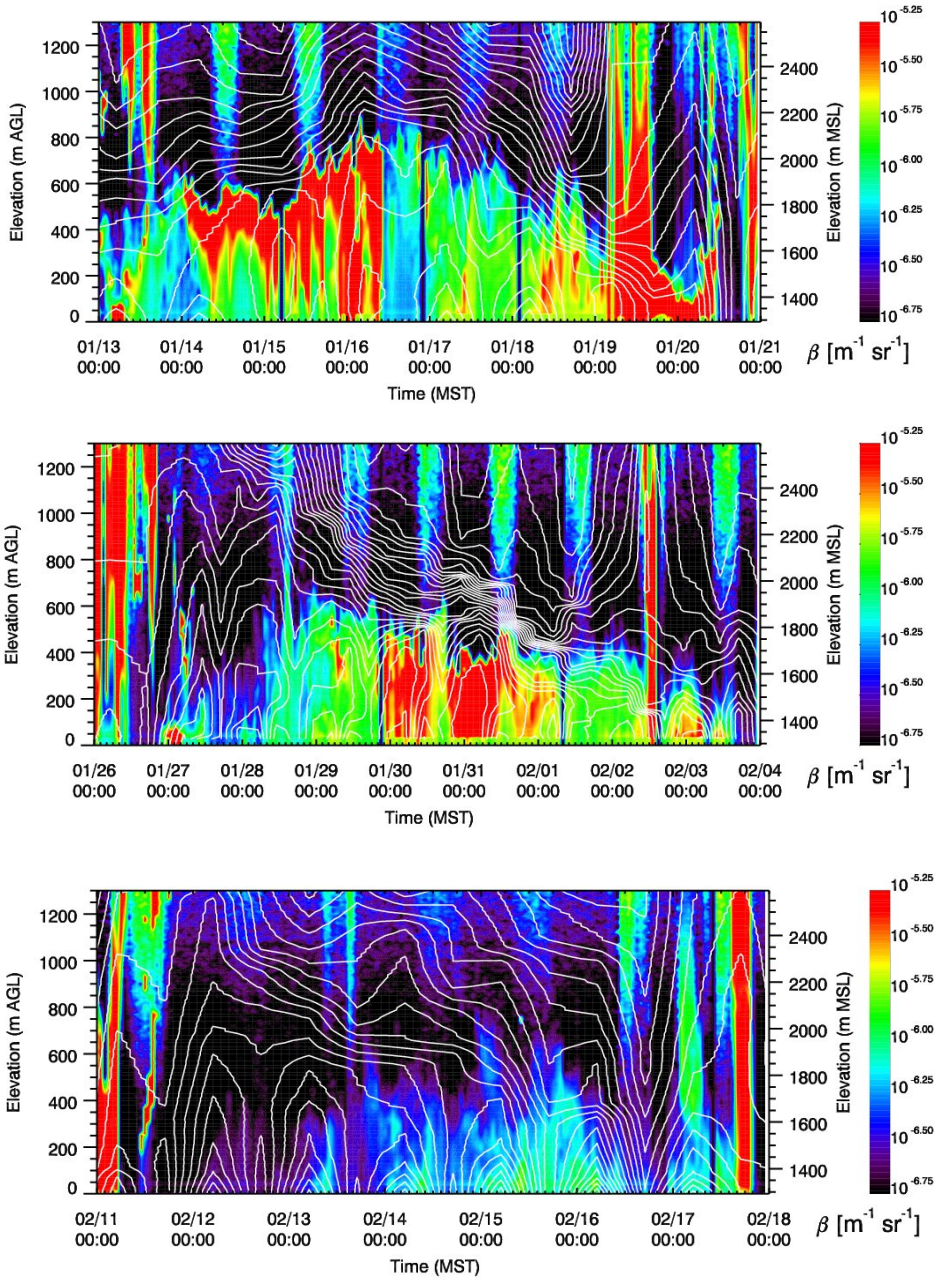

Figure 4: Time-height cross sections of ceilometer backscatter profile and contours of isentropes at the Landfill Site (LFL) in the Salt Lake Basin for three of the pollution episodes in early 2017. Isentropes are from KSLC radiosonde dataset. Note that some intermittent power outages occurred at the site.

4. Meteorological Analysis - Exchange Processes

The meteorological analysis was centered on the relevant meteorological exchange processes (see **Fig. 5**) within a PCAP in the Salt Lake Valley, between a PCAP and the free atmosphere, between different basins, and between the atmosphere over the Great Salt Lake and the Salt Lake Valley. Some of the scientific questions this study aimed to address include:

- What is the role of thermally driven circulations along valley sidewalls and through tributary canyons?
- How do these exchange processes influence air quality and the availability of precursor gases and reactants?

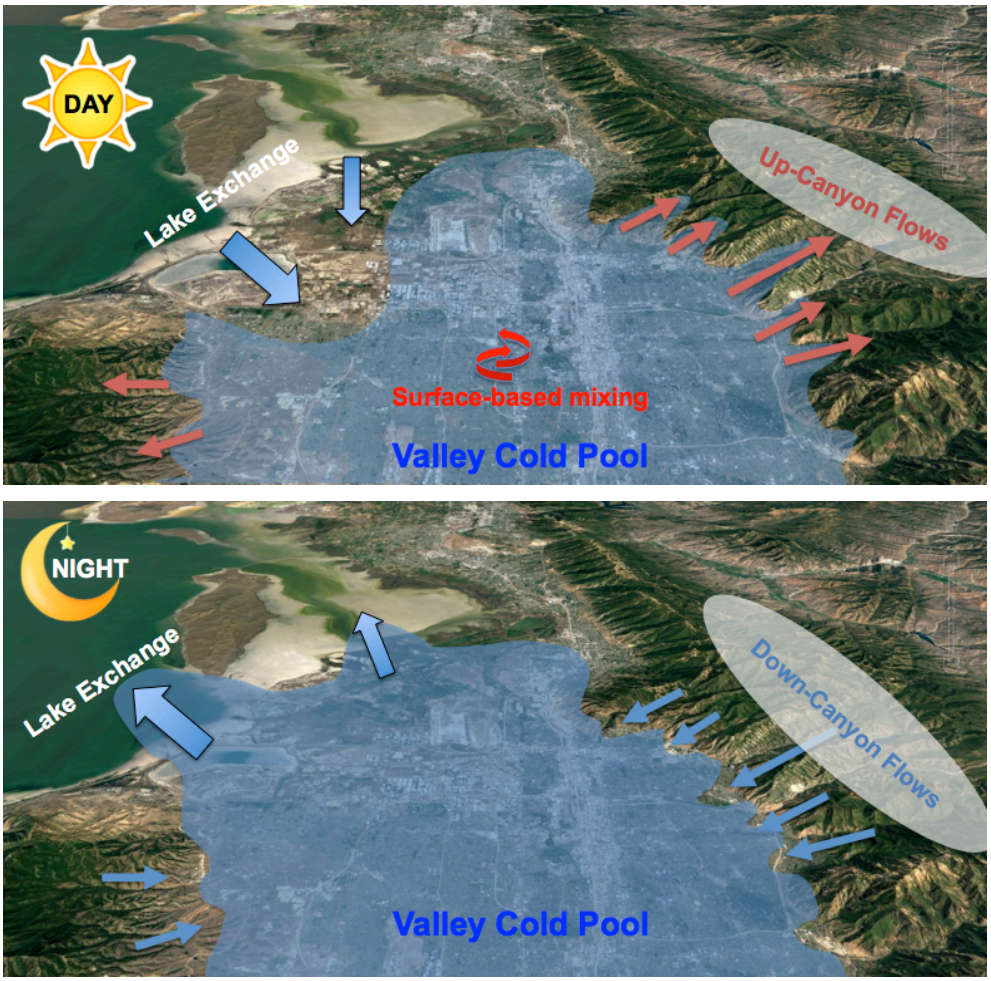

Figure 5: Schematic Illustration of diurnal exchange processes affecting the evolution of a PCAP in the Salt Lake Valley.

The NSF-funded meteorological component of UWFPS allowed the installation of equipment at the interfaces between the Salt Lake Valley and two tributary canyons (Red Butte Canyon and Parleys Canyon) and between the Salt Lake Valley and the Great Salt Lake. Further, LiDAR and radiosonde observations monitored the evolution of the thermal and dynamic structure of the PCAP at the center of the basin.

The Red Butte Canyon site (RB) was equipped with surface wind sensors, a ceilometer, and $PM_{2.5}$ and ozone observations, the Parleys Canyon (PAR) and Landfill (LFL) sites were augmented with additional SoDAR wind profilers. The goal was to investigate the link between up-canyon or down-canyon thermally driven flows at RB and PAR, particulate pollution, and ozone concentrations. Further, the role of air mass exchange with the boundary layer over the Great Salt Lake - both through thermally driven lake breezes and synoptically forced flows - was targeted with the observations at LFL and NAA. Insufficient funding was obtained to target meteorological inter-basin exchange processes but careful analysis of existing data sets such as Mesowest (Horel et al. 2002) allows for a limited characterization of these flows.

In the following, examples of these various exchange processes are highlighted through selected case studies.

4.1 Down-Canyon Flows

Thermally driven down-canyon flows are strongest during clear nights and synoptically quiescent conditions, when radiative surface cooling is strong and synoptic pressure gradients are weak. The onset of the 25 January to 4 February 2017 pollution episode was characterized by increasing influence of cloudiness from 27 January (clear) to 30 January (strong influence of cloud cover), reducing the effectiveness of night-time radiative cooling (not shown) in these initial days. Thermally driven flows were observed during the three nights at both the Parleys and Red Butte Canyon exits, as illustrated in **Fig. 6** (winds in down-canyon directions, 110 and 70 degrees, respectively) However, the strength of the flows decreased with increasing cloud effects (see wind speeds).

Winds at HW and UU also show signatures of diurnal thermal wind forcing, with nocturnal northeasterly downslope and daytime west-southwesterly upslope flows at UU and nighttime southeasterly and daytime northwesterly down- and up-valley flows. The near-surface wind speeds, however, are highest during the day and suggest a downward transport of momentum from aloft, while wind speeds are highest during the night at the canyon exits.

The time series of $PM_{2.5}$ and ozone are shown in the bottom panels of **Fig. 6**, and indicate a reduction in particulate concentrations and an increase in ozone concentrations during the night when the down-canyon flows transport aerosol scarce and ozone-rich air into the PCAP.

Thermally driven down-canyon flows are expected to occur on clear nights within all tributary canyons leading into the Salt Lake, Utah and Cache Valleys. These include the Bells Canyon, Little Cottonwood, Big Cottonwood, Parley Canyon, Mill Creek, Red Butte, and City Creek drainages in the Salt Lake Valley, Weber and Ogden Canyons to the north of Salt Lake City, and the Provo and American Fork Canyons in Utah Valley. Strong influences of drainage flows are expected through Logan and Blacksmith Canyons in Cache Valley. The relative strength of the canyon flows and how far and at what height above the Valley floors they extend into the PCAP atmosphere is largely unknown but likely a complex function of basin depth, slope, land cover, and other meteorological factors such as thermal stratification and the strength of synoptic flow. Signatures of possible injections of aerosol-scarce air reaching the HW site in the Salt Lake

Basin, and the Lindon site in Utah Valley can be found in the ceilometer backscatter profiles collected at these sites (not shown).

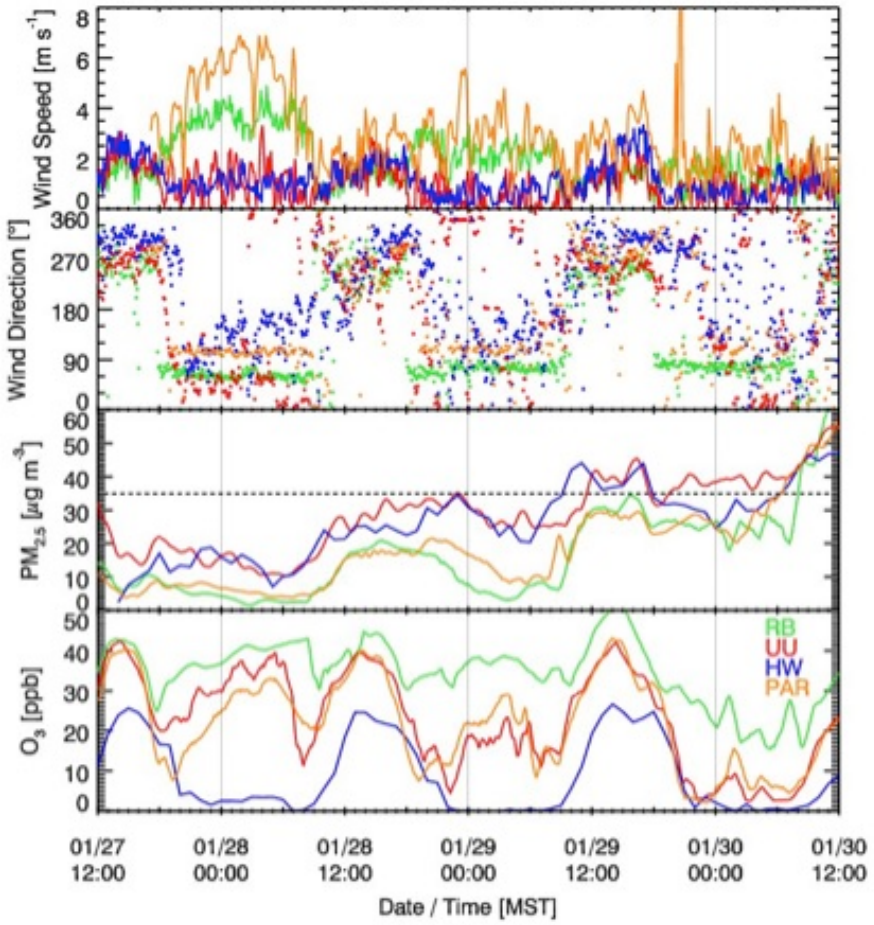

Figure 6: Time series of wind speeds, wind direction, $PM_{2.5}$ and ozone concentrations collected at four selected sites near the mouths of tributary canyons (PAR, RB), the valley sidewall (UU) and the basin floor (HW) during the onset of a particulate pollution episode.

4.2 Daytime Sidewall Ventilation - 29 January 2017

Even under PCAP conditions, a convective boundary layer (CBL) develops at the basin floor and along the basin sidewall during daytime. The depth of the convective mixing strongly depends on the surface net radiation, and thus on surface snow cover and cloud conditions. The development of the CBL can be seen in the vertical and pseudo-vertical temperature profiles (Section 2.1), ceilometer backscatter profiles (Section 2.3), and lidar-retrieved σ_w (Section 2.5).

Surface heating on the sun-exposed northeastern basin sidewalls is expected to drive upslope and up-canyon flows. While these flows were not directly targeted in the meteorological observations, they can be seen in time series of wind speed and direction at the canyon exit sites (PAR, RB, see **Fig. 6**). The thermal forcing, however, can be inferred from the difference between the balloon-based temperature soundings and the pseudo-vertical temperature profiles collected along the northeastern basin transect, as shown for the afternoon of 29 January 2017 (**Fig. 7b**). The LiDAR backscatter collected at HW during this day shows the growth

of the CBL (**Fig. 7c**). Aerosols ventilated along the basin sidewall are recirculated with the easterly flow above 2000 m ASL and are picked up in the backscatter profile at HW after 1400 MST.

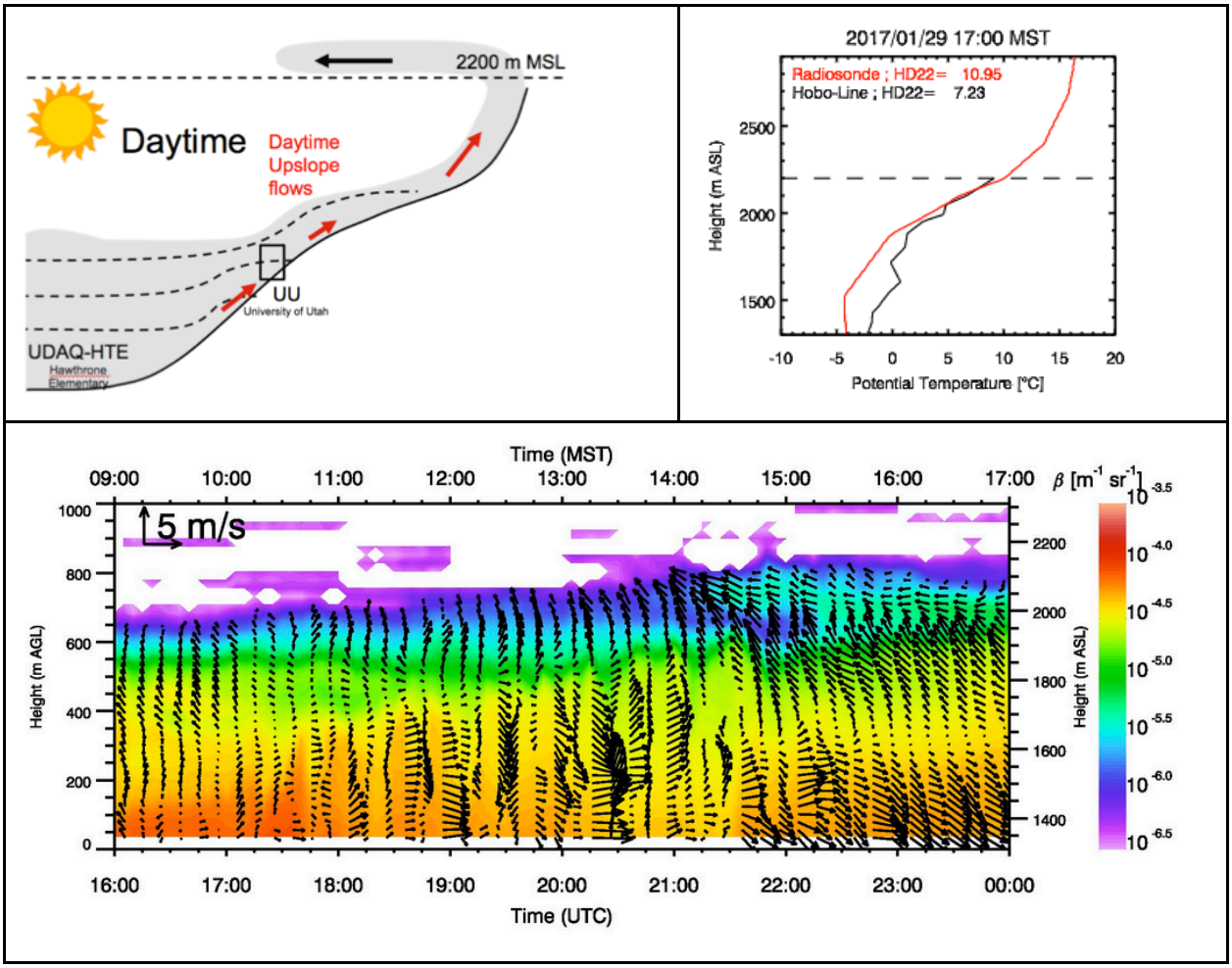

Figure 7: Illustration of basin sidewall ventilation on 29 January 2017. A schematic of the process is shown in the top left panel. Vertical (red) and pseudo-vertical temperature profiles (black) are shown for 1700 MST in the top right. The evolution of the convective boundary layer is shown in the lidar backscatter (bottom). The recirculation of sidewall-ejected aerosols at ~2050 m ASL reaches HW shortly after 1400 MST.

4.3 Lake Breeze Circulation - 30 January 2017

A lake-breeze event is illustrated in **Fig. 8** using the case study of 30 January 2017 as a pollution episode evolved in the Salt Lake Valley. In the afternoon, the thermal contrast between a warmer valley boundary layer and the cold air over the lake forced a lake breeze front to penetrate into the northern part of the Salt lake Valley. The lake atmosphere brought aerosol-scarce air into the basin, leading to a decreasing $PM_{2.5}$ concentrations as the breeze advanced.

The flight of the instrumented KSL-TV news helicopter (Crosman et al. 2017) flown in the northern part of the valley revealed the depth of the lake breeze. The last panel of **Fig. 8** shows

a smoothed profile of the averaged $PM_{2.5}$ observations as the helicopter ascended within and descended back into the PCAP. It reveals how shallow the lake breeze is as it undercuts the more heavily polluted valley airmass.

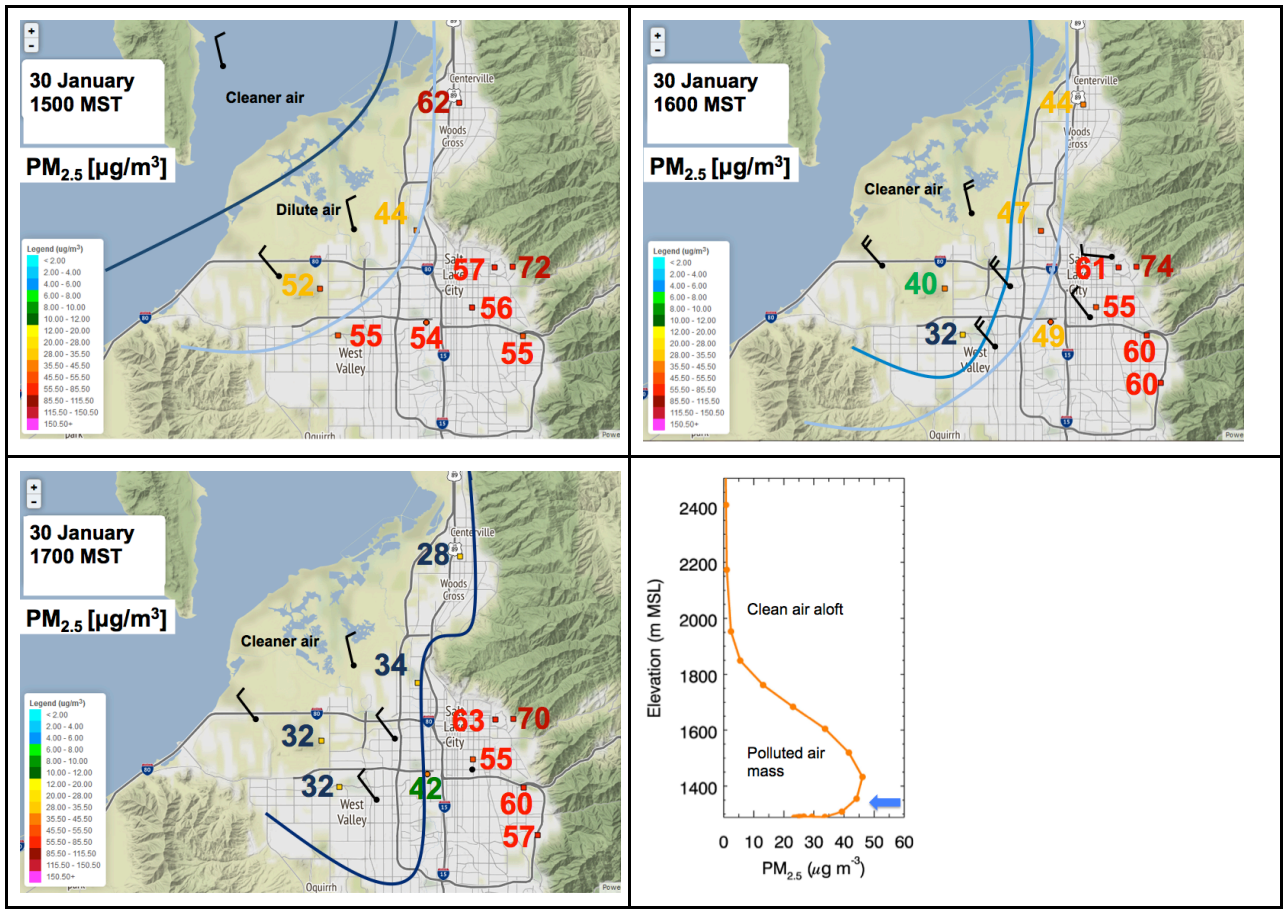

Figure 8: Analysis of the surface wind field and surface $PM_{2.5}$ concentrations during the 30 January 2017 lake breeze event. The last panel shows a smoothed vertical profile of $PM_{2.5}$ concentrations from observations on the KSL-TV news helicopter taken in the northern part of the basin.

4.4 Synoptically-Forced Lake Exchange

A schematic of the wind field and particulate concentrations during a synoptically-forced lake exchange event is shown in **Fig. 9**. In the morning of 3 February 2017, strong southerly flow scoured out the pollution from the Salt Lake basin, starting at the benches (0500 MST), and eventually eroding the entire PCAP in the basin (0730 MST). Polluted air was pushed north over the Great Salt Lake.

By 0900 MST, however, the flows weakened and colder and aerosol-rich air penetrated back into the lowest areas of the Salt Lake basin, leading to a "recharge" of the pollution are those locations. The last panel shows a photograph of the pollution tongue penetrating back into the basin.

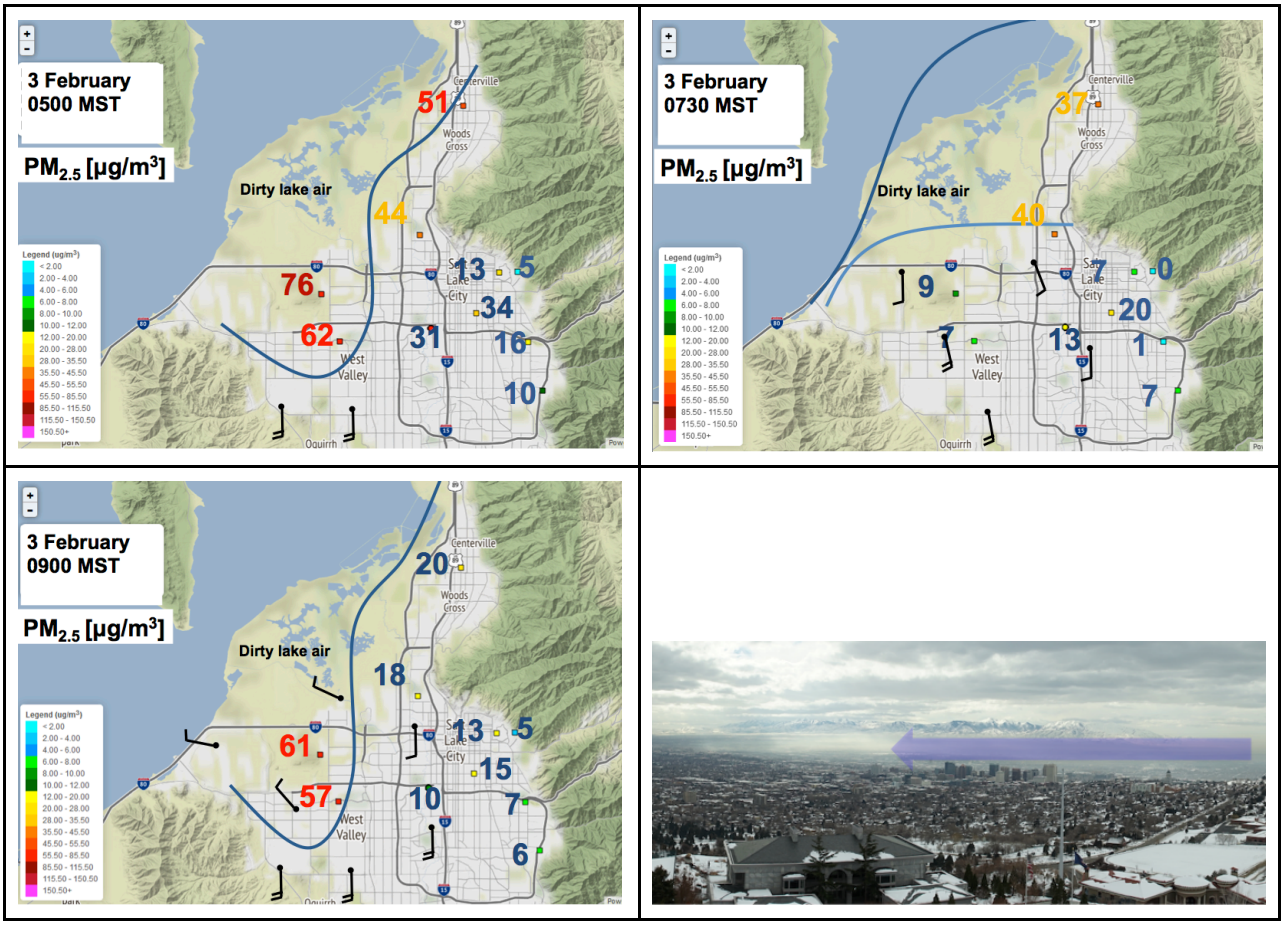

Figure 9: Analysis of the surface wind field and surface PM2.5 concentrations during the 3 February 2017 lake "recharge" event. The last panel shows a photograph of the shallow tongue of polluted air "recharging" the basin.

4.5 Inter-Basin Exchange

Inter-basin exchange through synoptically forced and or thermally driven circulations may play an important role in the import and export of pollutants, pollutant precursors, and oxidants. Initial plans to place additional equipment at the Jordan Narrows could not be realized due to limited funding. Nevertheless, data from MesoWest stations, TRAX-based measurements, and large gradients in pollutants between the Salt Lake and Utah Basins can indicate the role of such inter-basin exchange processes.

Initial analysis shows that elevated ammonia concentrations at HW are associated with periods of inter-basin exchange. During most nights during the UWFPS study, a period of southerly flow was observed by a Utah Department of Transportation Weather station in the Jordan Narrows gap (**Fig. 10**). However, periods when that exchange persisted for longer time periods were also observed. The following periods were identified as having both a PCAP and significant prolonged south-to-north (from Utah Valley into Salt Lake Valley) from Mesowest observations (**Fig. 11**): January 17-20, 28-31 and Feb 1-2 2017.

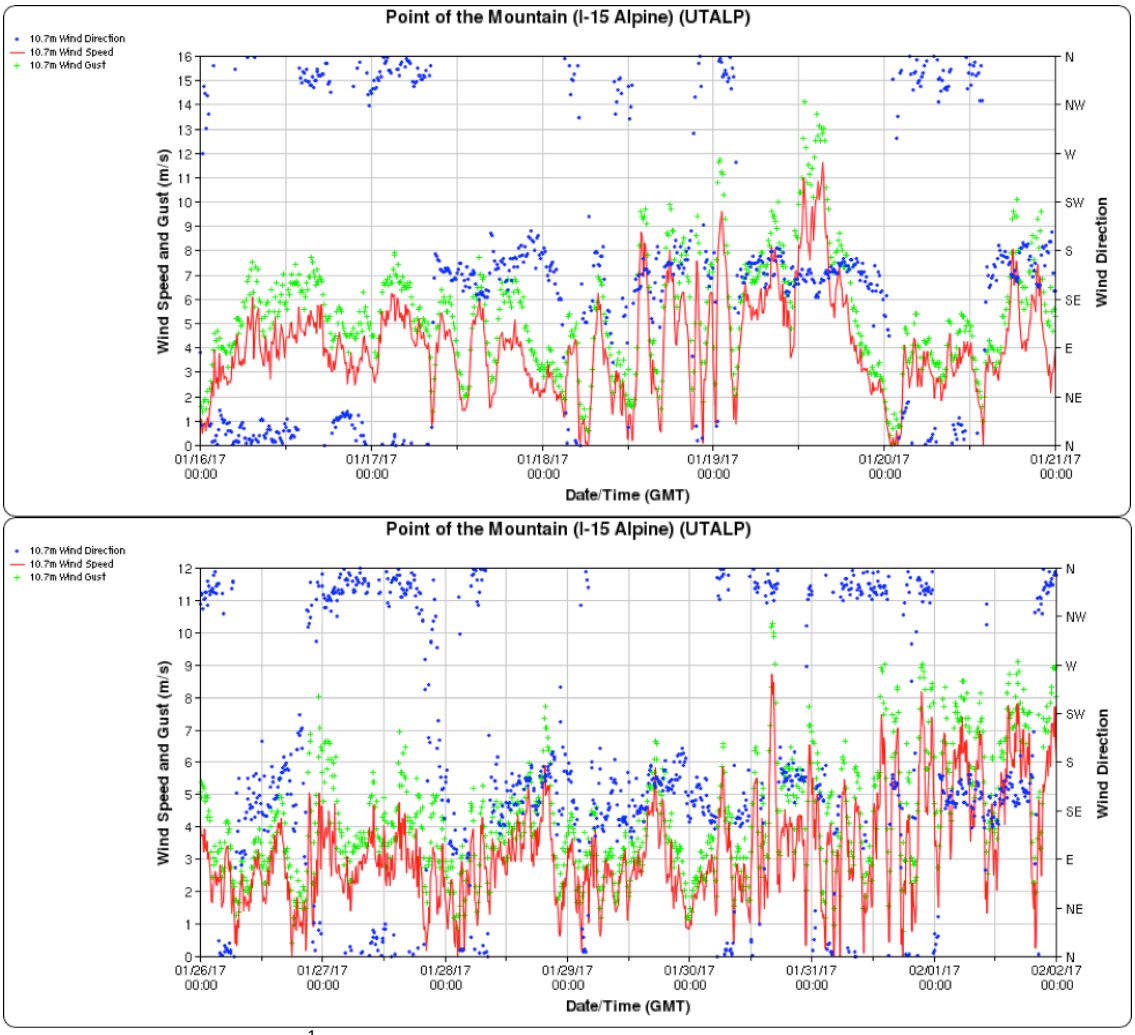

Figure 10: Wind speed (m s^{-1}) and wind direction at the Point of the Mountain Utah Department of Transportation weather station between 16-21 January 2017 (top) and 26 January - 2 February 2017 (bottom).

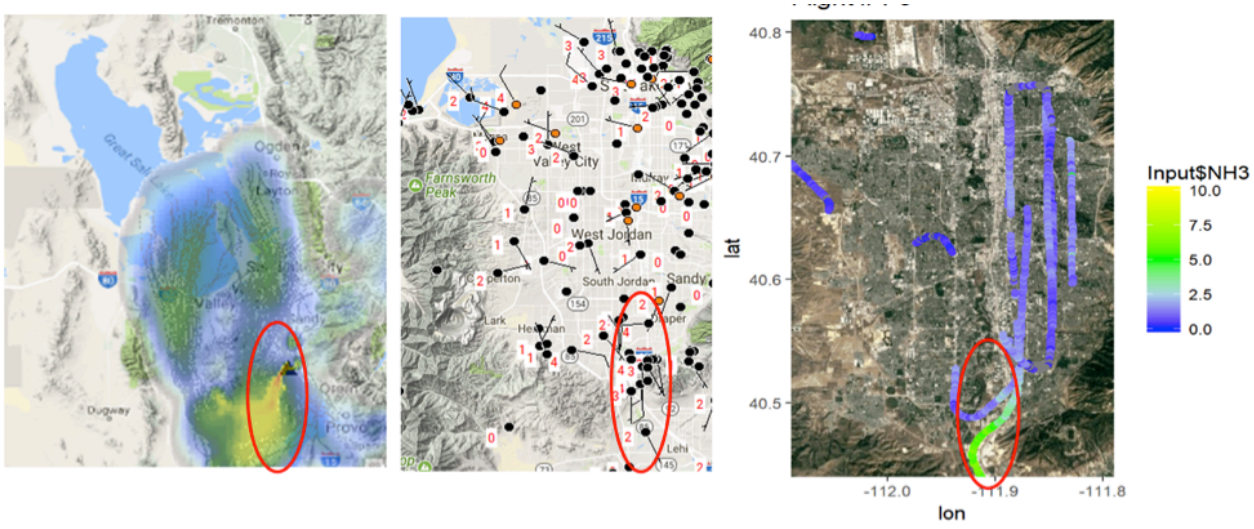

Figure 11: Analysis of HRRR-STILT backward trajectories (left panel), Mesowest surface wind speeds (middle panel, barb and red value, in ms^{-1}) and ammonia concentrations from the NOAA Twin Otter during the afternoon of 17 January 2017. The red circled region indicates the region of southerly inter-basin from the Utah Valley into the Salt Lake Valley and the associated high ammonia concentrations (ammonia figure courtesy Ann Middlebrook).

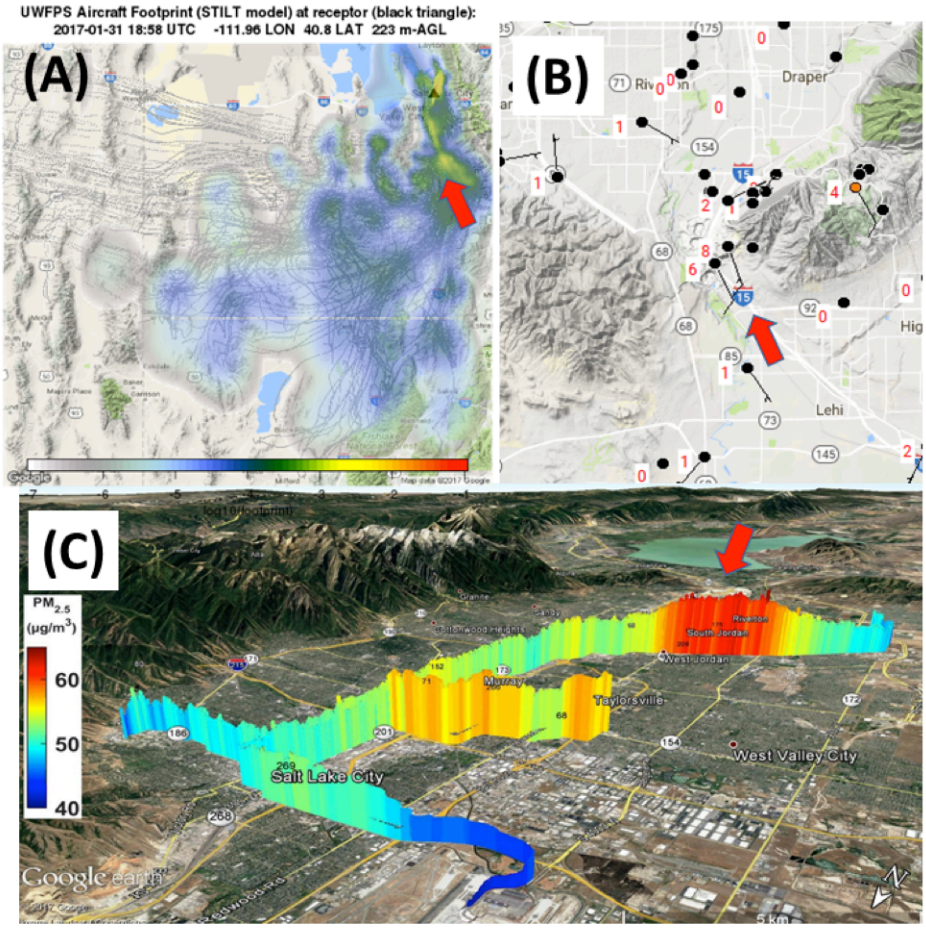

Figure 12: (a) analysis of HRRR-STILT backward trajectories, (b) Mesowest surface wind speeds (barb and red value, in ms^{-1}), and (c) TRAX $PM_{2.5}$ concentrations during mid-morning hours on 31 January 2017.

Another valuable resource for determining the southerly flow are particulate and ozone sensors onboard the TRAX light-rail train (Mitchell et al. 2017). On 31 January 2017, the TRAX sensors intersected a plume of air with higher particulate concentrations flowing into the Salt Lake Valley from the Utah Valley. Mesowest observations and HRRR-Stilt analyses verify that the source of the polluted air observed by TRAX was from the Utah Valley (**Fig. 12)**.

5. Weather Forecasts and Briefings

Daily weather briefings were prepared for UWFPS planning and posted every morning on the forecast website: http://uwfps.blogspot.com/. All archived forecasts and model and satellite imagery shown in the forecasts remains available on the blog site. On some days, discussion presentations were given to the science team and presented in person at the airport hangar or meeting rooms at the University of Utah and Utah Division of Air Quality. The forecasts were

provided for the Salt Lake, Utah, and Cache Valleys and were tailored to fit the specific needs of the NOAA aircraft planning team. See the forecast products at http://uwfps.blogspot.com/ for more information on the various weather parameters that were provided.

5.1 Daily Weather Forecast Briefings

In-person 10-20 minute weather briefings were prepared for science team meetings using a forecast funnel approach (large scale to small scale). 24-7 forecast support was provided via a private cell phone line as visibility conditions changed rapidly and frequent support updates were needed.

5.2 Forecast Products

The forecast products were disseminated in the daily weather briefings as well as through a ½-1 page forecast summary and discussion uploaded daily to to http://uwfps.blogspot.com/ and also be sent out each day via email. The forecasts focused on PCAP structure and evolution. Specifically**:** PCAP start and end times and detailed PCAP characteristics (depth, intensity, cloud cover, fog, visibility, ceiling height, wind speed, and temperature).

5.3 Forecast Funnel Approach

The forecasts consisted of the following components:

a) Long-term outlook, 5-8 days before: upper-level evolution.

b) Mid-term outlook, 2-4 days before: upper-level evolution, winds aloft and in boundary layer, cloud cover and visibility, PCAP intensity and depth, surface conditions (snow cover, lake temperature).

c) Short-term outlook 6-36 hours before: All the components in 2), with the addition of greater forecast specificity for spatial and temporal variations in cloud cover, visibility, PCAP vertical structure, and outlook for lake-induced flows, canyon and slope flows.

d) Nowcast, 0-6 hr before: All of the components in 2) and 3), with the addition of observational products (i.e., ceilometers, lidar, Mesowest, satellite, etc) to diagnose the current conditions and to inform short-term changes in the PCAP structure and evolution.

5.4 Numerical and Observational Forecast Guidance

Several numerical models were used to provide forecasts, including (1) the local NOAA National Weather Service Weather Research and Forecast (WRF) model, (2) the National Center for Environmental Prediction (NCEP) Global Forecasting System (GFS), (3) the NCEP High Resolution Rapid Refresh Model (HRRR), (4) the NCEP North American Model (NAM), and (5) the NCEP Short Range Ensemble Forecast (SREF) model suite. These numerical model forecasts were supplemented with all available observational networks (e.g., snow depth observations, ceilometers, lidar, KSL-TV news helicopter and TRAX observations, radiosondes, satellite imagery) in order to provide the highest accuracy of short-term forecasts possible.

6. Online Resources

Visualizations of the various datasets are available for reference and download via the following links:

Overview over basic meteorology and selected chemical species:

- http://www.inscc.utah.edu/~hoch/AIRQUAL_2016-2017/AWS/TimeSeriesMeteo.pdf

Overview over Lidar-retrieved winds at the HW site:

- http://www.inscc.utah.edu/~hoch/AIRQUAL_2016-2017/LIDAR_HW/

Overview over ceilometer-derived aerosol backscatter profiles (some EPA operated):

- HW site: http://www.inscc.utah.edu/~hoch/AIRQUAL_2016-2017/CEILOMETER/HW/
- LFL site: http://www.inscc.utah.edu/~hoch/AIRQUAL_2016-2017/CEILOMETER/LFL/
- RB site: http://www.inscc.utah.edu/~hoch/AIRQUAL_2016-2017/CEILOMETER/MTN/
- PAR site: http://www.inscc.utah.edu/~hoch/AIRQUAL_2016-2017/CEILOMETER/PAR/
- LOG site: http://www.inscc.utah.edu/~hoch/AIRQUAL_2016-2017/CEILOMETER/LOG/
- UTV site: http://www.inscc.utah.edu/~hoch/AIRQUAL_2016-2017/CEILOMETER/UTV/

Overview over SoDAR-retrieved winds at the LFL and PAR site:

- PAR site: http://www.inscc.utah.edu/~hoch/AIRQUAL_2016-2017/SODAR_PAR/
- LFL site: http://www.inscc.utah.edu/~hoch/AIRQUAL_2016-2017/SODAR_LFL/

Forecast Blog

- http://uwfps.blogspot.com/

7. Acknowledgements

We would like to thank all UWFPS collaborators for a constructive field experiment. Other non-funded University investigators contributed through extensive discussions, sharing of data, and equipment loans. We would like to thank all volunteers who housed equipment on their property, especially Wim Cardoen, The Salt Lake Country Club, and Brad Leinberger.

8. References

Baasandorj, M., S. W. Hoch, R. Bares, J. C. Lin, S. S. Brown, R. Martin, K. Kelly, D. B. Millet, K. J. Zarzana, W. P. Dube, G. Tonnesen, J. Sohl, C. D. Whiteman: 2017: Coupling between Chemical and Meteorological Processes under Persistent Cold-Air Pool Conditions: Evolution of Wintertime PM2.5 Pollution Events and N2O5 Observations in Utah's Salt Lake Valley, Environmental Science & Technology 2017 *51* (11), 5941-5950; DOI: 10.1021/acs.est.6b06603

Crosman, E. T., and J. D. Horel, 2016: Winter lake breezes near the Great Salt Lake. *Boundary-Layer Meteorol.*, 159, 439-464.

Crosman, E. T., and J. D. Horel, 2017: Large-eddy simulations of a Salt Lake Valley cold-air pool. Submitted to *Atmospheric Research*.

Foster, C., E. T. Crosman, and J. D. Horel, 2016: Simulations of a cold-air pool in Utah's Salt Lake Valley: Sensitivity to land use and snow cover. Accepted for publication in *Boundary-Layer Meteorol.*

Hall, S. J., G. Maurer, S. W. Hoch, R. Taylor, D. R. Bowling, 2014: Impacts of anthropogenic emissions and cold air pools on urban to montane gradients of snowpack ion concentrations in the Wasatch Mountains, Utah. *Atmos. Environ.*, **98**, 231-241

Hoch, S. W., E. T. Crosman, M. Baasandorj, J. C. Lin, R. Bares, R. S. Martin, J. Sohl, J. D. Horel, and C. D. Whiteman, 2016: Case Study of the 6-16 February 2016 Salt Lake Valley Persistent Cold-Air Pool. 17th Conference on Mountain Meteorology, 27 June – 1 July 2016 Burlington, VT. Available at: https://ams.confex.com/ams/17Mountain/recordingredirect.cgi/id/34698?entry_password=519479&uniqueid=Paper296260

Holmes, H. A., J. K. Sriramasamudram, E. R. Pardyjak, and C. D. Whiteman, 2015: Turbulent fluxes and pollutant mixing during wintertime air pollution episodes in complex terrain. *Environ. Science Techn.*, **49**(22),13206-13214.

Lareau, N. P., E. T. Crosman, C. D. Whiteman, J. D. Horel, S. W. Hoch, W. O. J. Brown, and T. W. Horst, 2013: The Persistent Cold-Air Pool Study. *Bull. Amer. Meteor. Soc.,* 94, 51–63.

Lareau, N. P., and J. D. Horel, 2015a: Dynamically Induced Displacements of a Persistent Cold-Air Pool. *Boundary-Layer Meteorol.*, 154, 291–316.

Lareau, N. P., and J. D. Horel, 2015b: Turbulent Erosion of Persistent Cold-Air Pools: Numerical Simulations. *J. Atmos. Sci.,* 72, 1409-1427.

Lu, W., and S. Zhong, 2014: A numerical study of a persistent cold-air pool episode in the Salt Lake Valley, Utah. *J. Geophys. Res. Atmos.*, 119:1733-1752

Silcox, G. D., K. E. Kelly, E. C. Crosman, C. D. Whiteman, and B. L. Allen, 2012: Wintertime PM2.5 concentrations during persistent, multi-day cold air pools in a mountain valley. *Atmos. Environ*., 46, 15-24.

Whiteman, C. D. and S. W. Hoch, 2014: Pseudo-vertical temperature profiles in a broad valley from lines of temperature sensors on sidewalls. *J. Appl. Meteor. Climatol.*, **53**, 2430–2437.

Whiteman, C. D., S. W. Hoch, J. D. Horel, A. Charland, 2014: Relationship between particulate air pollution and meteorological variables in Utah's Salt Lake Valley. *Atmos. Environ*., **94**, 742-753..

Young, J. S., and C. D. Whiteman, 2015: Laser ceilometer investigation of persistent wintertime cold-air pools in Utah's Salt Lake Valley. *J. Appl. Meteor. Climatol*., 54, 752-765

Zardi D., Whiteman C.D., 2013: Diurnal Mountain Wind Systems. In: Chow F., De Wekker S., Snyder B. (eds) Mountain Weather Research and Forecasting. Springer Atmospheric Sciences. Springer, Dordrecht